

High Strain Rate Blow Formability of Newly Developed Al-Mg-High-Mn Alloy

Tomoyuki Kudo

Akira Goto

Kazuya Saito

Abstract : Blow forming accompanied with superplasticity makes possible the forming of complex parts, which cannot be formed by cold press forming. The conventional superplastic AA5083 alloy 'ALNOVI®-1' developed by the Furukawa-Sky Aluminum Corp. shows high superplasticity because of its fine grain and is widely used for blow forming. However, for mass production of components, an Al-Mg alloy with finer-sized grains is needed. In this research, the newly developed high Mn version of the Al-Mg alloy 'ALNOVI-U' is used, and this material possesses grains finer than those of the conventional AA5083 alloy. The effects of finer grain size on the blow formability at high strain rates over 10^{-2} /s and the properties of the resulting moldings were studied.

1. Introduction

The 2000 and 7000 series aluminum alloys, which have fine grains and show high superplasticity, are used for special components such as those used in aircraft, and are used as materials for blow forming. It is relatively difficult to ensure fine grains in the 5000 series aluminum alloys and the superplasticity is slightly inferior. However, the 5000 series aluminum alloys have high corrosion resistance and weldability; therefore, these alloys are in great demand as materials for blow forming common components. The Furukawa-Sky Aluminum Corp. has developed the superplastic AA5083 alloy 'ALNOVI-1' with a fine grain size of 10 μm or less by a proprietary process and ALNOVI-1 is widely used globally. ALNOVI-1 shows not only high superplasticity at low strain rates but also good elongation at high strain rates, as is required for high productivity. However, there was a need for a material suitable for higher strain rate blow forming, because the 5000 series aluminum alloys came to be used for mass production items. Therefore, the Furukawa-Sky Aluminum Corp. developed the Al-Mg-Mn alloy 'ALNOVI-U' which allows for grains to be made 2 μm smaller by adjusting the amount of additive Mn¹⁾ and attempts were made to enhance elongation at high strain rates (10^{-2} - 10^{-1} /s). In this study, the

potential of ALNOVI-U was evaluated by investigating in detail the effects of finer grain size on high-temperature tensile properties, blow formability, and properties of moldings formed at high strain rates (10^{-2} - 10^{-1} /s).

2. Experimental

2.1 Materials

The chemical composition of the tested alloy ALNOVI-U used in the experiments and AA5083 alloy are shown in **Table 1**. The sample alloy was subjected to DC-casting, homogenization, and hot and cold rolling. The thickness of cold rolled sheet was 0.5 mm. The precipitates in the tested alloys and AA5083 are shown in **Fig. 1**. The precipitates in ALNOVI-U are more densely distributed because the amount of additive Mn is higher than that in AA5083. It is thought that these precipitates contribute to the decrease in grain size by stabilizing grain boundaries and acting as nucleation sites for recrystallization. The cold rolled sheet of ALNOVI-U was

Table 1 Chemical composition. (mass%)

Material	Si	Fe	Mn	Mg
ALNOVI-U	0.03	0.05	1.42	4.75
AA5083	0.03	0.04	0.73	4.70

annealed and the grain size of the sheet's alloy were manipulated to be 6 μm ; this is finer than that of AA5083, 9 μm which is equivalent to that of AA5083 and 13 μm which is coarser than that of AA5083. These samples are called '6 μm ' sample, '9 μm ' sample, '13 μm ' sample respectively in this paper. The grain structures are shown in Fig. 2.

2.2 High temperature tensile tests

Tensile tests were conducted at 663 K, 703 K and 743 K. The deformation resistance and elongation at high temperatures were measured by tensile tests at constant strain rates of 10^{-3} , 10^{-2} and $10^{-1}/\text{s}$. The deformation mechanisms at high temperatures were studied by analyzing the results of the strain rate change tensile tests in the range 10^{-4} to $10^{-1}/\text{s}$.

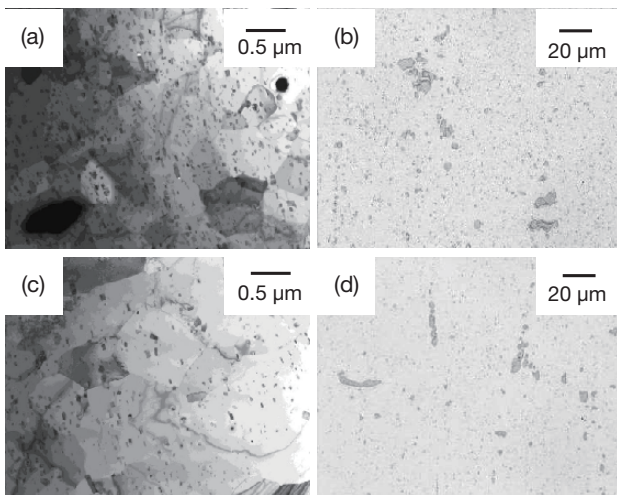


Fig. 1 Precipitates in ALNOVI-U and AA5083.

- (a) Fine precipitates observed by TEM in ALNOVI-U.
- (b) Coarse precipitates observed by SEM in ALNOVI-U.
- (c) Fine precipitates observed by TEM in AA5083.
- (d) Coarse precipitates observed by SEM in AA5083.

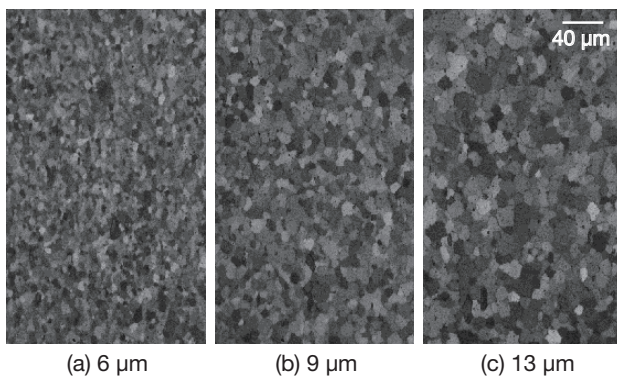


Fig. 2 Grain structures of ALNOVI-U manipulated by annealing. They were subjected to the experiments.

2.3 Blow Forming tests

After the sheets were inserted between the mold plates, heated in the blow forming machine, and kept hot for 10 min, blow forming by N_2 gas was conducted. The mold shape was similar to that of an automobile quarter panel. The blow forming machine used in the experiments can exert high pressure in a few seconds and is therefore suitable for high strain rate blow forming. In this research, high strain rate blow forming tests that are quicker than conventional tests were conducted; the forming times were 5, 10, 15, and 20 s. The gas pressure in these tests was constant at 3 MPa, and the temperatures were 663 K, 703 K and 743 K.

2.4 Molding Properties

(a) Appearance

The moldings were inspected for breaks. In addition, the molding accuracy was evaluated by measuring the radius of curvature at the point that is formed at the end of the forming as shown in Fig. 3.

(b) Cavitation

For evaluating cavitation volume, sections with different thickness reductions were selected from the moldings and polished. The cavitation area ratio was determined using an area analyzer. In addition, the strain distribution in grains around the cavitations was observed by electron backscatter diffraction (EBSD).

(c) Grain structure and strength after forming

The grain structures in the selected sections were observed by Barker's method and the initial and final grain sizes were measured. In addition, the Vickers hardness of these sections was measured.

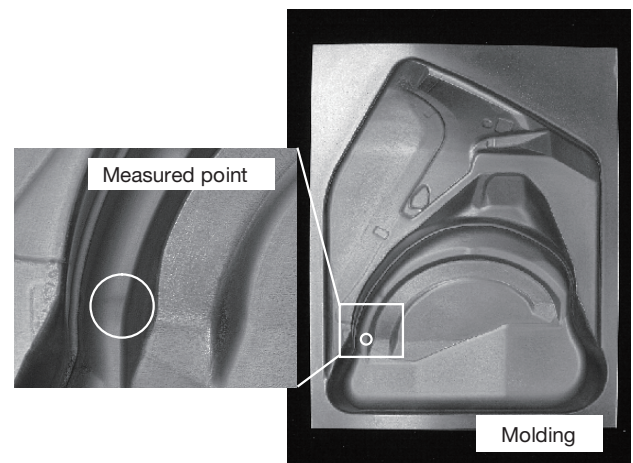


Fig. 3 Molding and measured point of curvature radius.

3. Results and Discussion

3.1 Deformation resistance and elongation at high temperature

The stress-strain curves for constant strain rates are shown in Fig. 4. At any strain rate, the deformation resistance of the 6 μm sample was the smallest. Comparing the characteristics of the S-S curves, in particular, for the 9 μm and 13 μm samples, a large peak was observed in early deformation and the deformation resistance increased with the strain rates. In contrast, for the 6 μm sample the peak was small, even at strain rates of $10^{-2}/\text{s}$. In addition, in the 6 μm sample, the deformation resistance was small and the typical S-S curves in grain boundary sliding situations, which have a large n value, were remarkably visible, even at strain rates of $10^{-2}/\text{s}$.

The elongations of each sample are shown in Fig. 5. The sample with finer grains showed greater elongation, especially at strain rates lower than $10^{-2}/\text{s}$. The elongation of each sample converged at lower temperatures or higher strain rates. The difference between the elongations of the 9 μm and 13 μm samples decreased at strain rates greater than $10^{-2}/\text{s}$. Furthermore, the effect of grain size diminished at strain rates

of $10^{-1}/\text{s}$. However, the 6 μm sample showed a larger elongation than the other samples even at strain rates in the range 10^{-2} – $10^{-1}/\text{s}$, which are higher than those used in conventional blow forming.

3.2 Discussion of deformation mechanism at high temperature

The relation between stress and strain rates, as deduced from measurements made in the course of strain rate change tensile tests, are shown in Fig. 6. The slope m indicates the strain rate sensitivity exponent. In each sample, m was approximately 0.5 at low strain rates and 0.3 at high strain rates. The relevant equation at high temperature is represented by Eq. (1)²⁾, where, $\dot{\epsilon}$ is the strain rate, A is a constant, k is the Boltzmann constant, T is the temperature, G is the shear modulus, b is the Burgers vector, d is the grain size, σ is the flow stress, p is the grain size exponent, D_0 is the diffusion constant, Q is the activation energy, and R is the gas constant. The m and p values of each deformation mechanism are summarized in Table 2²⁾⁻⁵⁾. From the values listed in Table 2, we deduced that grain boundary sliding occurs at low strain rates in the area of $m = 0.5$, and solute drag creep occurs at high strain rates in the area of $m = 0.3$. It is assumed that in

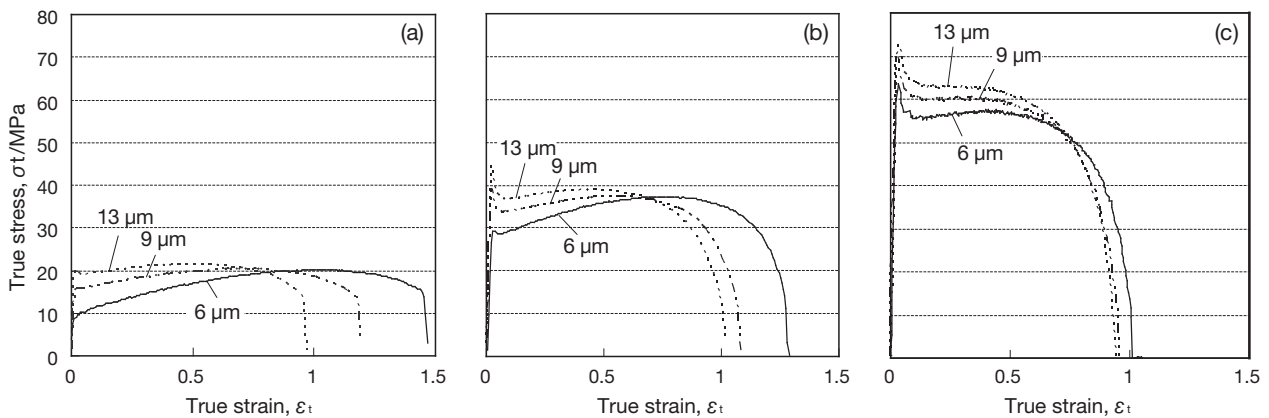


Fig. 4 S-S Curves measured by constant strain rate tensile tests (703 K).
(a) $10^{-3}/\text{s}$, (b) $10^{-2}/\text{s}$, (c) $10^{-1}/\text{s}$.

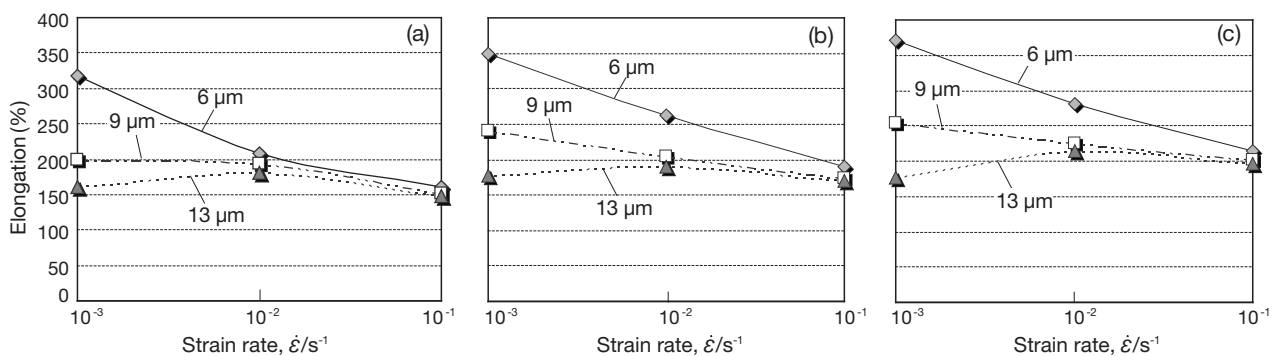


Fig. 5 Elongation as measured in constant strain rate tensile tests.
(a) 663 K, (b) 703 K, (c) 743 K.

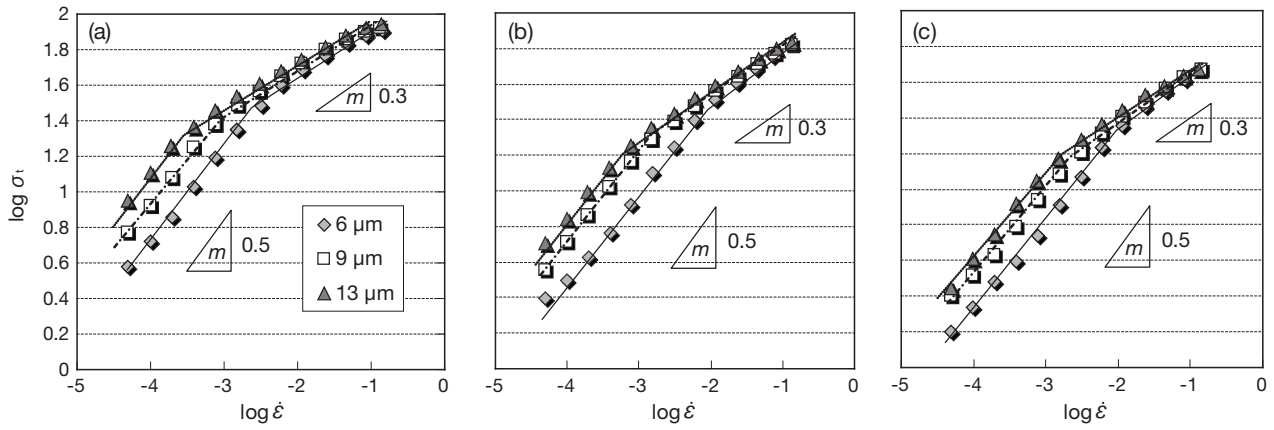


Fig. 6 Strain rate sensitivity exponents measured by strain rate change tensile tests. (a) 663 K, (b) 703 K, (c) 743 K.

Table 2 m and p value of deformation mechanism at high temperature.²⁾⁻⁵⁾

		m	p
Diffusional creep	Nabarro-Herring creep	1	2
	Coble creep	1	3
Grain-boundary sliding	Lattice diffusion	0.5	2
	Grain-boundary diffusion	0.5	3
Dislocation creep	Harper-Dorn creep	1	0
	Solute drag creep	0.33	0
	Climb-controlled creep	0.2	0

this alloy, deformation proceeds with interaction between the dislocation and the solute Mg. in the area of $m = 0.3$. It is found that grain boundary sliding occurs even at higher strain rates at higher temperature or finer grain size (see Fig. 5). The shift in the value of strain rate at which grain boundary sliding occurs when the grain size becomes finer from 9 μm to 6 μm is simply estimated by Eq. (1). It is found that it is shifted to an approximately 2.3-3.4 times higher strain rate because p is 2-3 (see Table. 2).

$$\dot{\epsilon} = A \left(\frac{Gb}{kT} \right) \left(\frac{b}{d} \right)^p \left(\frac{\sigma}{G} \right)^{1/m} D_0 \exp \left(-\frac{Q}{RT} \right) \quad (1)$$

The 6 μm sample shows the smallest deformation resistance and the largest elongation even at high strain rates in the range 10^{-2} - 10^{-1} /s because grain boundary sliding contributes at higher strain rates in this sample. However, the contribution of grain boundary sliding is small and that of solute drag creep is large at strain rates over 10^2 /s in coarse grained samples. It is thought that the large peak shown in the S-S curves are generated by interactions between dislocations and solute Mg, causing an increase in deformation resistance at high temperature. From Eq. (1) and Table. 2, grain boundary sliding is affected by grain size d and solute drag creep is not,

because p is 0. It is thought that the reason why elongation of each sample converged at a strain rate 10^{-1} /s is that the deformation mechanism of whole materials become one of solute drag creep.

From the results of the test pieces described above, the contribution of grain boundary sliding is made larger and therefore large elongation and low deformation resistance is shown, even at low temperature and high strain rates, by using ALNOVI-U. It is expected that ALNOVI-U will enable the blow forming temperature and time to be reduced. The formabilities and properties of moldings obtained in high strain rate blow forming tests are shown below.

3.3 Appearance

The radius of curvature at the point formed in the end of the forming process as a function of the forming time is shown in Fig. 7. The symbol \times signifies that breaking occurred in the moldings. A small radius of curvature means that sharp edges can form faster and that there is good molding accuracy as shown in Fig. 8. Breaking was shown by the 13 μm sample as forming proceeded, but not in the 9 μm and 6 μm samples. From this result, it is confirmed that the samples of finer grain size have larger ductility, even at the high strain rates as those used in the forming tests. That corresponds to relation between grain size and elongation shown in Fig. 5. And it is found that the finer grains enable to form sharp edges faster or at lower temperature as shown in Fig. 7. This can be accounted for by the deformation resistance being smaller in the case of finer grains, even at high strain rates as shown in Fig. 4.

3.4 Cavitation

Cavitation area ratio as a function of thickness reduction of each part in the molding is shown in Fig. 9. Cavitation increased with thickness reduction, but the 6 μm sample

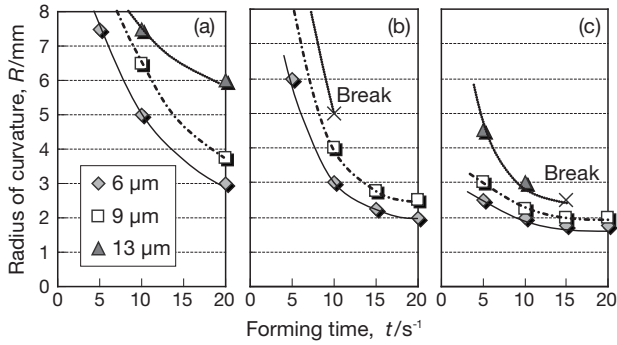


Fig. 7 Radius of curvature against forming time. (a) 663 K, (b) 703 K, (c) 743 K.

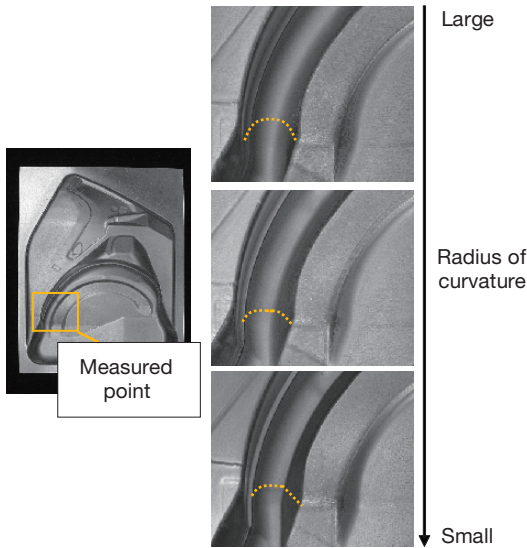


Fig. 8 Radius of curvature and appearance of molding.

showed the lowest values. Fig. 10 (a) shows the section at point D in Fig. 9 observed by a optical microscope. It is found that fewer cavitations were generated at finer grain sizes. Fig. 10 (b) shows an Image Quality map of the 6 μm and 13 μm samples observed by EBSD and it represents the average strain in the grains by means of a gray scale. It is confirmed that initial cavitations were generated on the triple junctions of grain boundaries by grain boundary sliding. In the 13 μm sample, the largely stretched grains accepting intragranular deformation are shown and it is assumed that the initial cavitations were combined and became larger along the grain boundaries. It is said that initial cavitations are generated by stress concentration on the triple junctions of grain boundaries or the interfaces of coarse precipitates⁶⁾.

However, it is thought that the distribution of precipitates are not largely difference because the chemical compositions of these samples are the same. Therefore, considering only the effect of grain size, it is assumed that initial cavitations tend to be generated because stress concentration occurs on the triple junctions of grain boundaries in the 13 μm sample and, in

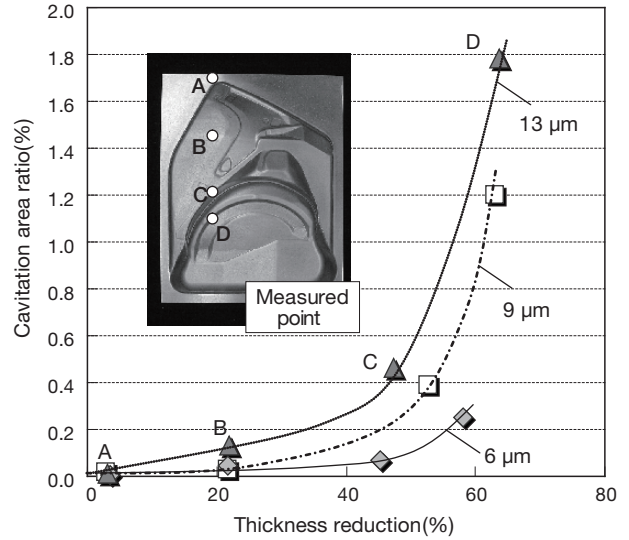


Fig. 9 Cavitation area ratio against thickness reduction. (Forming time is 10 s and forming temperature is 703 K.)

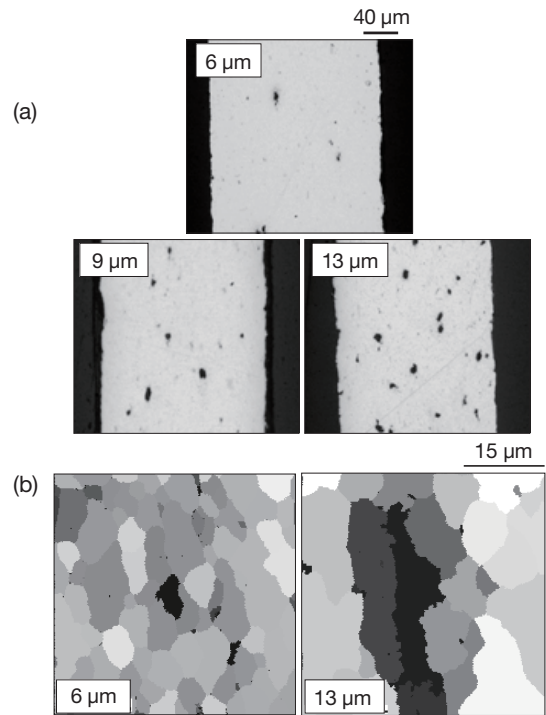


Fig. 10 Cavitation of each sample. (a) Image observed by optical microscope. (b) Image quality map observed by EBSD.

addition, initial cavitations tend to be larger because of intragranular deformation. It is thought that initial cavitations do not tend to be larger because the contribution of intragranular deformation is relatively small, and therefore the cavitation area ratio in the 6 μm sample is the lowest.

3.5 Grain structure and strength after forming

The relation between thickness reduction and grain size after forming is shown in Fig. 11. Point A represents the grain size not deformed, points B, C and D represent grain sizes at about the same points of B, C and D in Fig. 9 respectively.

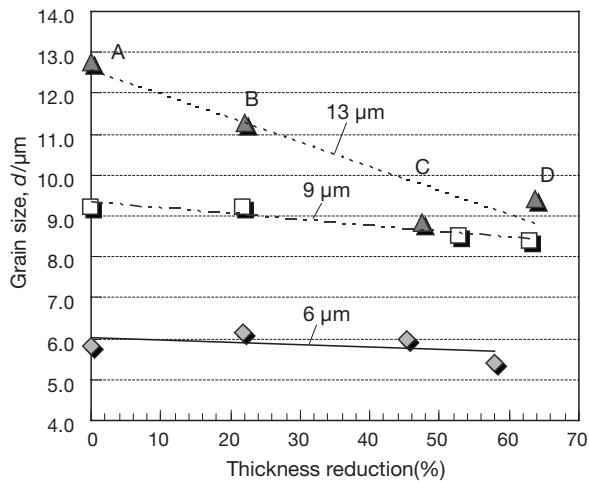


Fig. 11 Grain size after forming. (Forming time is 10 sec and forming temperature is 703 K.)

The grain sizes after forming were remarkably made finer as the initial grain size became coarser. The plots as the grain size becomes slightly larger are shown and the tendency for refinement of the grain size is less in the 6 μm and 9 μm samples. It is considered that this effect is due to the grain size being made finer by dynamic recrystallization because the contribution of intragranular deformation is larger as the grain size increases. The reason why the grain size becomes slightly larger in fine grain samples is thought to arise from the transfer of grain boundary, occurring by an accommodation process. However, the grain size after forming was finer as the initial grain size was finer (see Fig. 11). Fig. 12 shows the Vickers hardness of point B. The 6 μm sample has the largest hardness because it has the finest grain (Hall-Petch relationship).

4. Summary

ALNOVI-U containing high Mn, which has a grain size of 6 μm was used, and its high-temperature tensile properties, high strain rate blow formability, and properties of components in the samples with grain sizes of 6 μm, 9 μm, and 13 μm were studied. The temperatures in the tests conducted for this study were 663 K, 703 K and 743 K; the strain rates were greater than $10^{-2}/s$, and the following results were obtained.

- In the high temperature tensile tests, the sample which involves the finest grain size of 6 μm showed the highest elongation and the smallest deformation resistance because grain boundary sliding worked effectively even at strain rates in the range 10^{-2} - $10^{-1}/s$.
- Even in the high strain rate blow forming tests, involving a forming time of 10 s using the mold having the shape

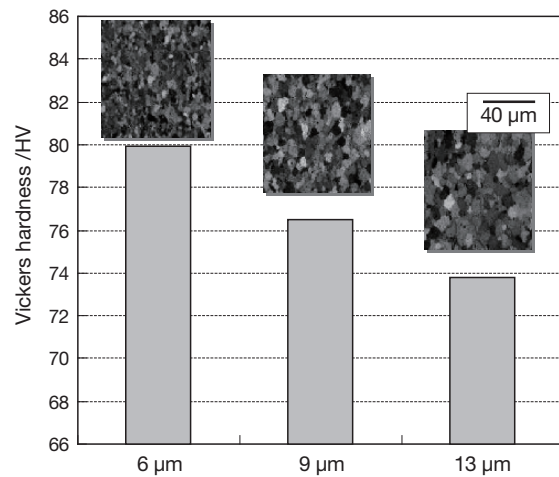


Fig. 12 Vickers hardness and microstructures of moldings against initial grain size.

of an automobile quarter panel model, breaking was not generated and the mold was able to form faster and at lower temperatures for the 6 μm sample.

- The molding made by the 6 μm sample showed the least cavitation and the largest hardness.

From the above, it is thought that ALNOVI-U facilitates blow forming at lower temperatures and shorter forming times, thereby rationalizing production and is, in addition, able to achieve the fabrication of components that are lighter but which have high strength. Effectiveness of ALNOVI-U to the automobile panel production was evaluated by Honda R&D Co., Ltd. and Honda Engineering Co., Ltd.

This article was published in Materials Science Forum, **735** (2013), 271. (www.scientific.net)

References

- 1) K. Ichitani and T. Tagata: Materials Science Forum, **539-543** (2007), 357.
- 2) H. Somekawa, H. Watanabe, M. Kohzu and K. Higashi: Materials Science Forum, **419-422** (2003), 393.
- 3) K. Kitazono: Journal of Japan Institute of Light Metals, **59** (2009), 458.
- 4) T. Ito, M. Ishikawa, M. Otsuka, M. Saga and M. Kikuchi: Journal of Japan Institute of Light Metals, **53** (2003), 114.
- 5) D. Oleg, E. M. Sherby and Eric M. Taleff: Materials Science and Engineering, **A322** (2002), 89.
- 6) H. Hosokawa, H. Iwasaki, T. Mori, T. Tagata, M. Mabuchi and K. Higashi: Journal of Japan Institute of Light Metals, **49** (1999), 57.



Tomoyuki Kudo
Technical Research Division
Furukawa-Sky Aluminum Corp.



Akira Goto
Automobile R&D Center
Honda R&D Co., Ltd.

Kazuya Saito
Body Die & Molding Engineering Division
Honda Engineering Co., Ltd.